Electronic Supplementary Material (ESI) for Sustainable Energy & Fuels.


# Self-shape-transformable 3D Tessellated Bifacial Crystalline Si Solar Cell Module for Extra Energy Gain through Intervals and an Integrated Actuator

**Min Ju Yun[1], Yeon Hyang Sim[1,2], Dong Yoon Lee[1] and Seung I. Cha*[1,2]**

**1. Energy Conversion Research Center, Electrical Materials Research Division, Korea Electrotechnology Research Institute**

**2. Department of Electro-functionality Materials Engineering, University of Science and Technology**

## Supporting Information

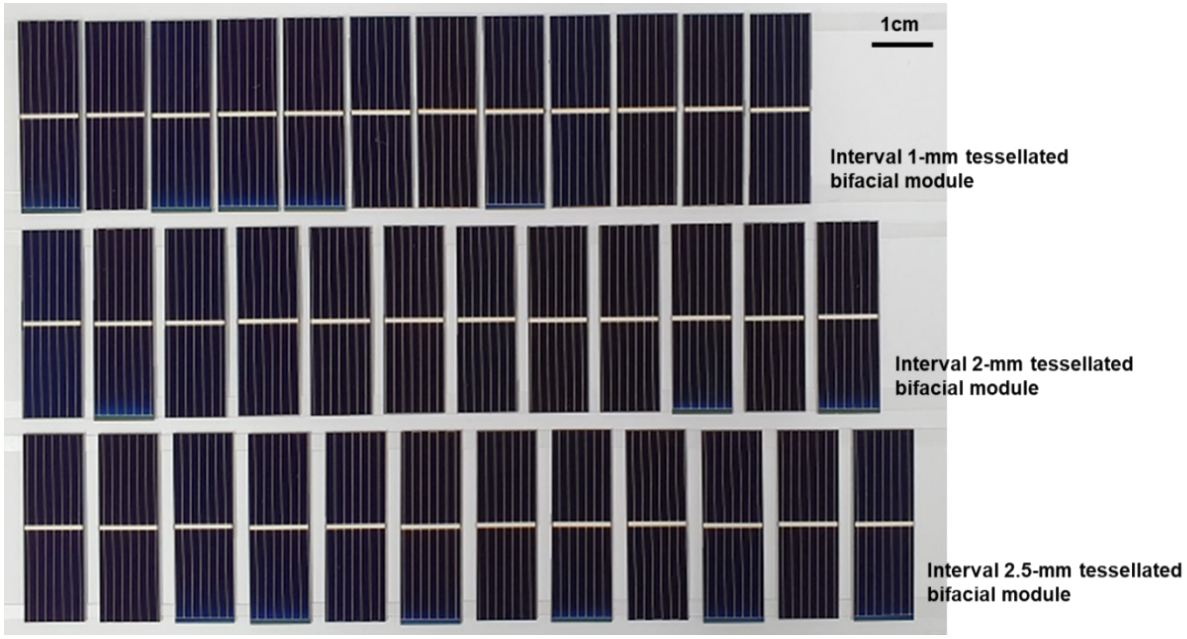


**Figure S1**. Photographs of flat tessellated bifacial modules with intervals of 1 mm (top), 2 mm (middle), and 2.5 mm (bottom).

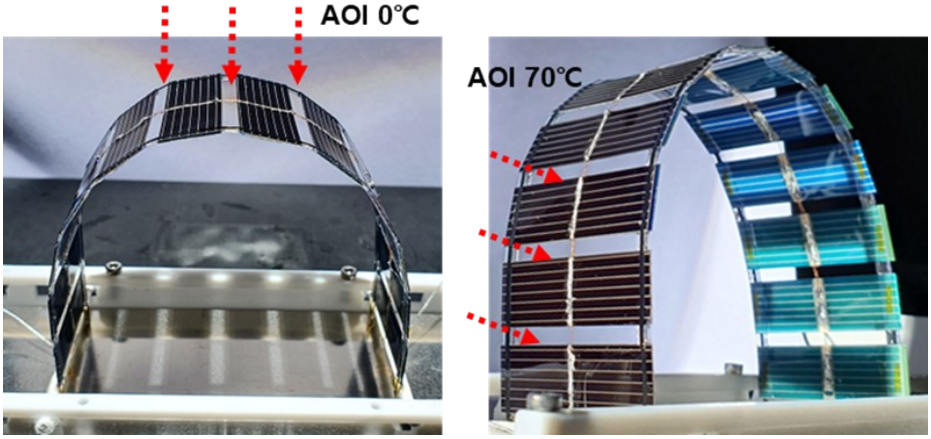


**Figure S2**. Photographs of a 3D arch tessellated bifacial module with a 2 mm interval, under directional incident light at an AOI of 70° and with a reflector.

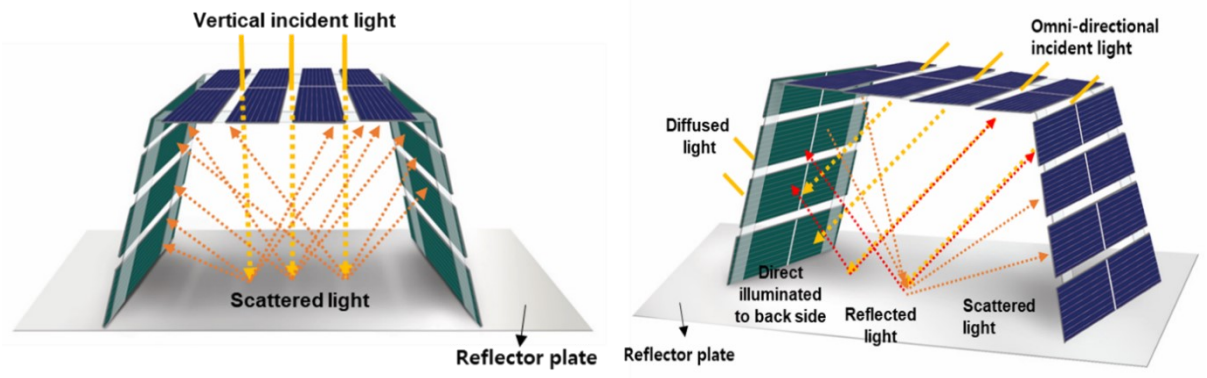


**Figure S3**. Schematic of the 3D tetragon tessellated bifacial module under vertical directional incident light (left side) and under omnidirectional incident light composed of reflected, scattered, and diffused light (right side) from the reflector through the intervals between cells.

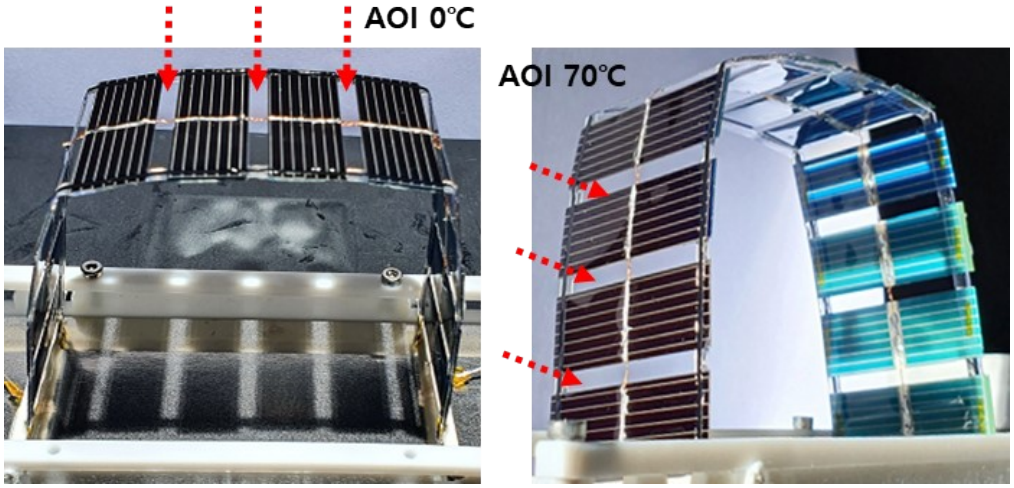


**Figure S4**. Photographs of the 3D tetragon tessellated bifacial module with 2 mm intervals, under directional incident light at an AOI of 70° and with a reflector.

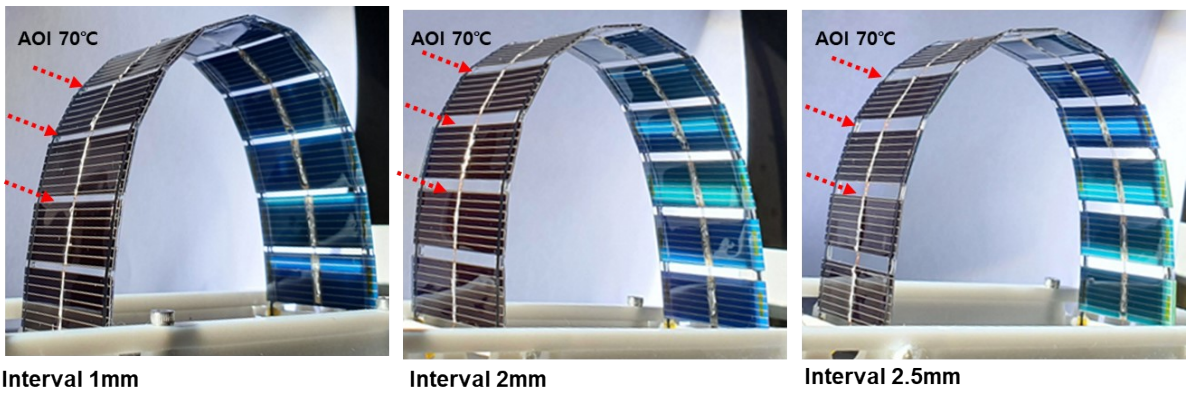


**Figure S5**. Photographs of the 3D arch tessellated bifacial module under omnidirectional incident light at an AOI of 70°, with an interval 1 mm (left), 2 mm (middle), or 2.5 mm (right) and without a reflector.

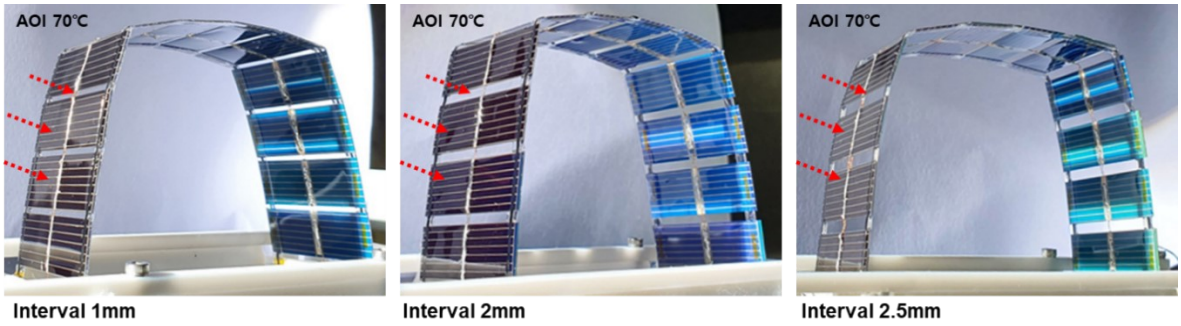


**Figure S6**. Photographs of the 3D tetragon tessellated bifacial module under omnidirectional incident light at an AOI of 70°, with an interval 1 mm (left), 2 mm (middle), or 2.5 mm (right) and without a reflector.

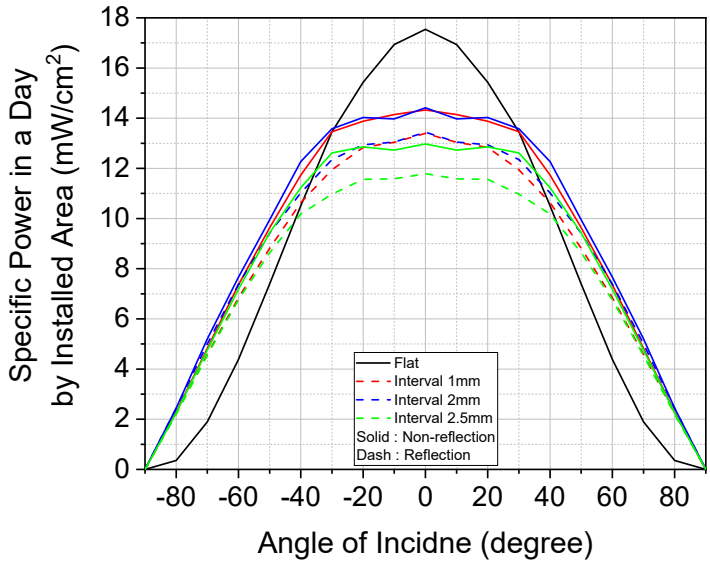


**Figure S7**. Specific power over the course of a day considering the installed area of 3D arch tessellated bifacial modules with various intervals and with or without a reflector.

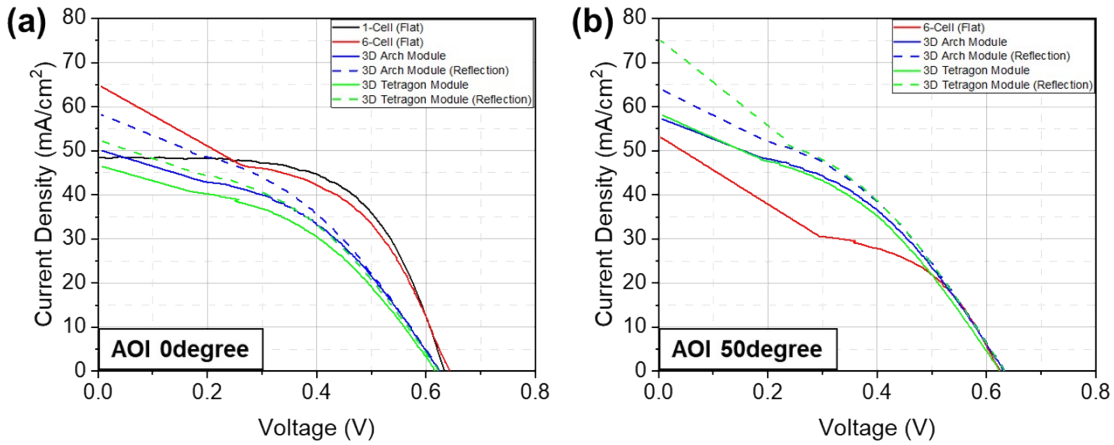


**Figure S8**. Relationship between voltage and current density of 1-cell and 6-cell flat module, 3D arch and tetragon tessellated bifacial module with and without reflection effect according to (a) AOI 0 degree and (b) AOI 50 degree.

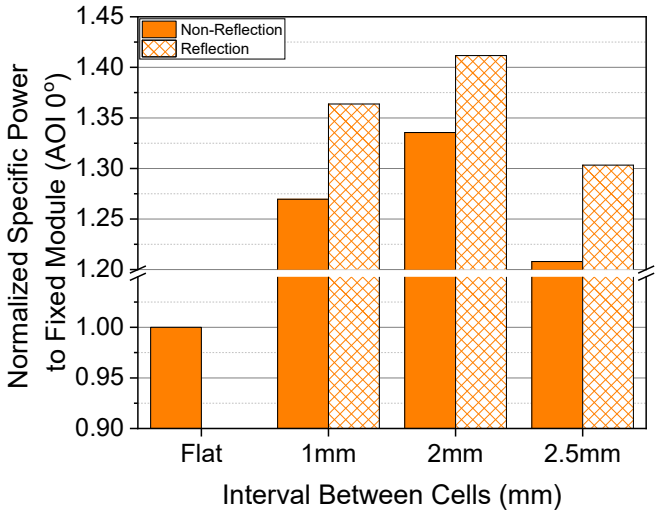


**Figure S9**. Accumulated specific power of the 3D arch tessellated bifacial module normalized to that of a flat module with various intervals and with and without a reflector.

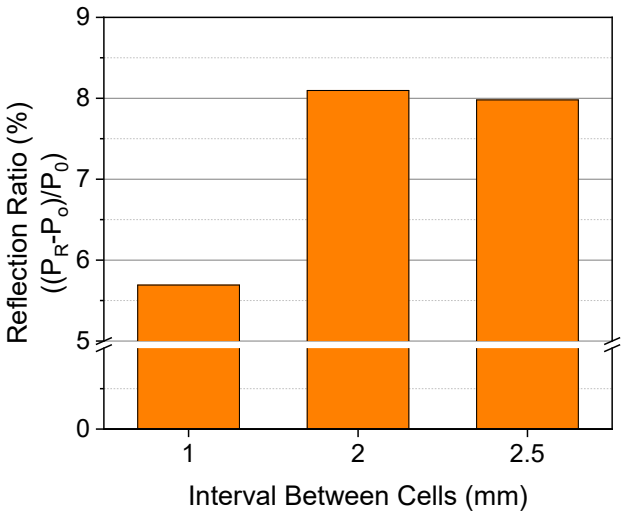


**Figure S10**. Reflection ratio of the 3D tetragon tessellated bifacial modules with various intervals between cells.

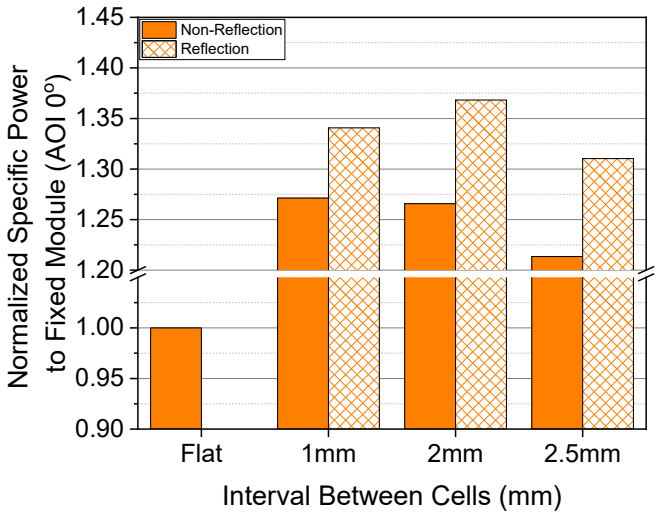


**Figure S11**. Accumulated specific power of the 3D tetragon tessellated bifacial modules normalized to that of a flat module, with various intervals and with and without a reflector.

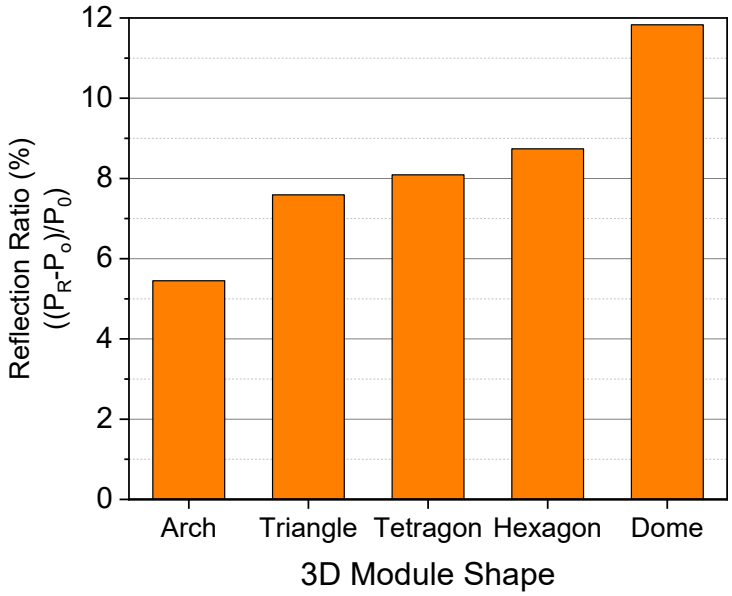


**Figure S12**. Reflection ratio of the 3D tessellated bifacial modules with an interval of 2 mm and with various 3D shapes.

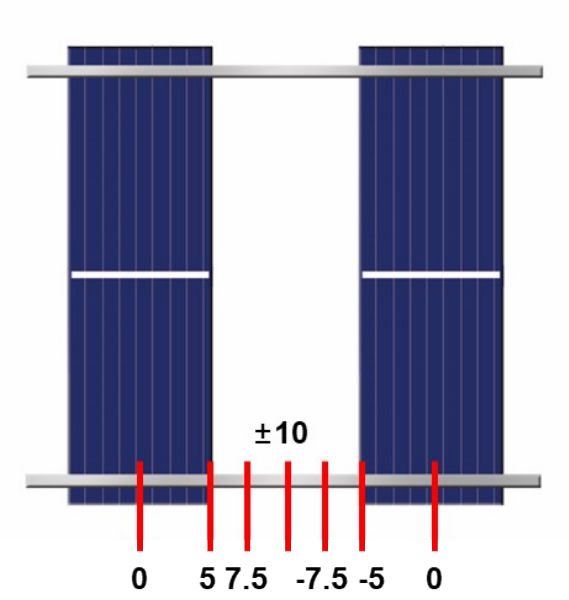


**Figure S13**. Schematic of the SMA surface temperature measured from the center of the cell to the center of the interval between two cells.

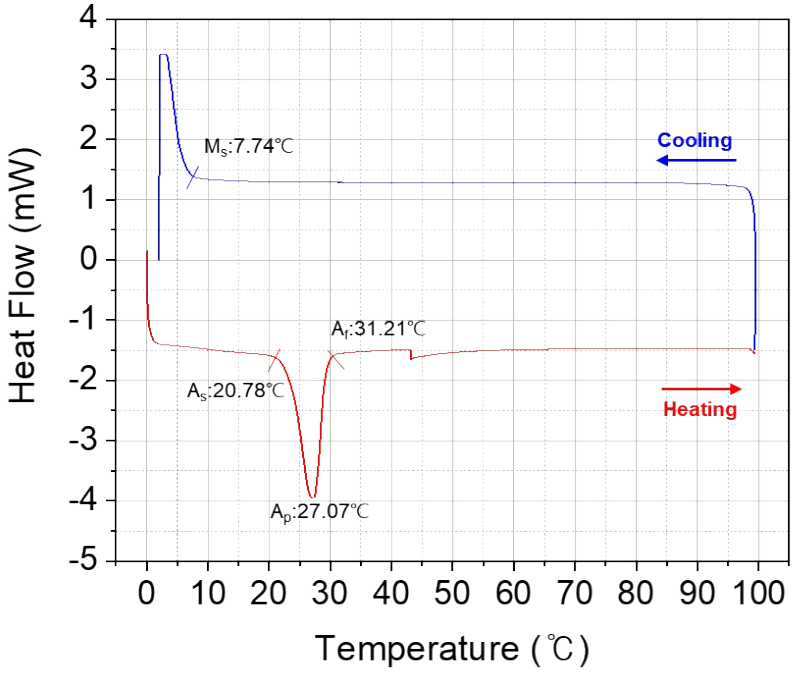


**Figure S14**. Differential scanning calorimetry (DSC) analysis of the shape memory alloy used as an actuator.

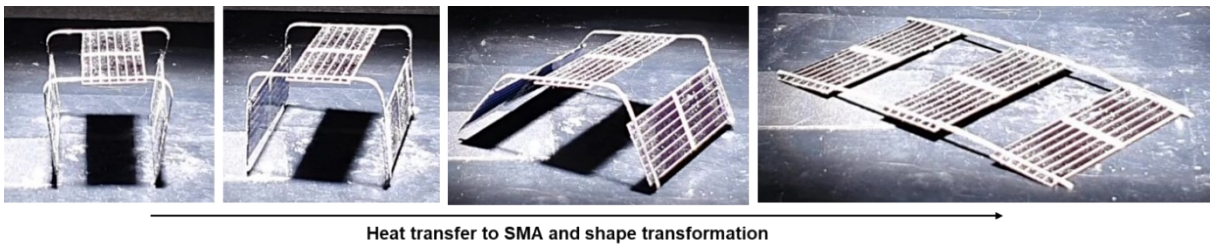


**Figure S15**. Photographs of the transformation process of three rectangular bifacial cells arranged from folded to flattened shapes under 1 Sun illumination.

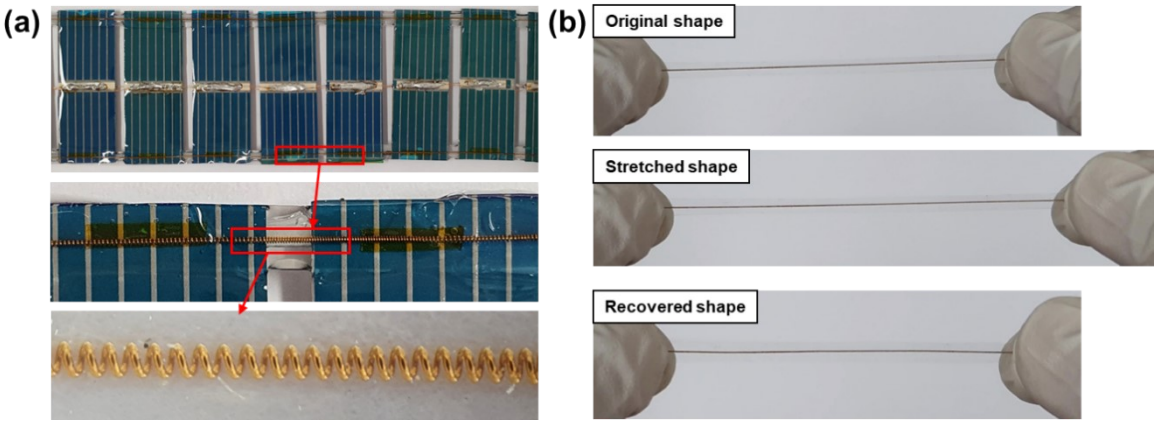


**Figure S16**. Photographs of (a) the backbone elastic strip with an embedded microspring and (b) the backbone's deformation and recovery.

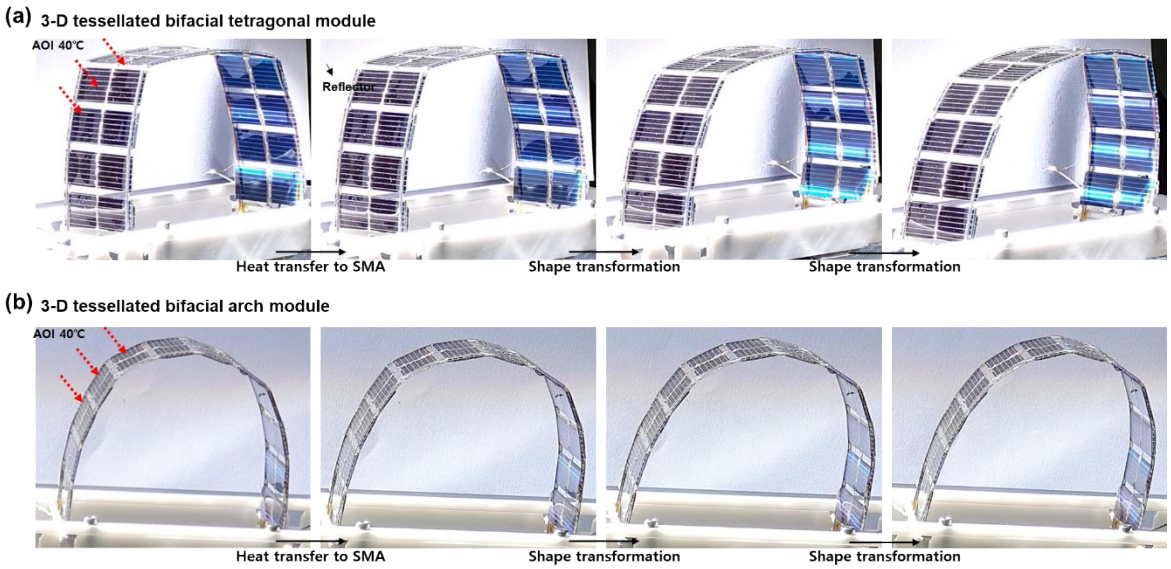


**Figure S17**. Photographs the transformation process of (a) a 3D tetragon tessellated bifacial module (top) and (b) a 3D arch tessellated bifacial module (bottom) under omnidirectional illumination at an AOI of 40°.

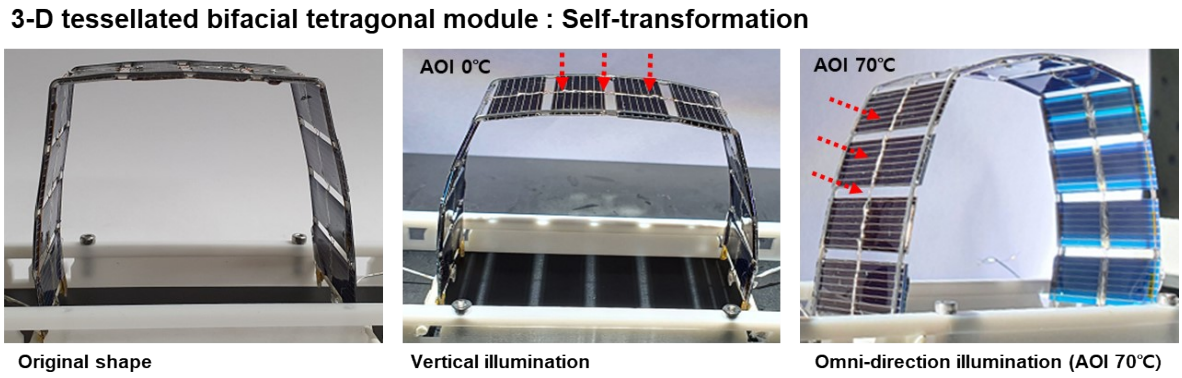


**Figure S18**. Photographs of the self-shape-transformable 3D tetragon tessellated bifacial module's completed transformed shape under the nonilluminated state (original shape, left), under vertical directional incident light (middle), and under omnidirectional incident light at an AOI of 70° (right).

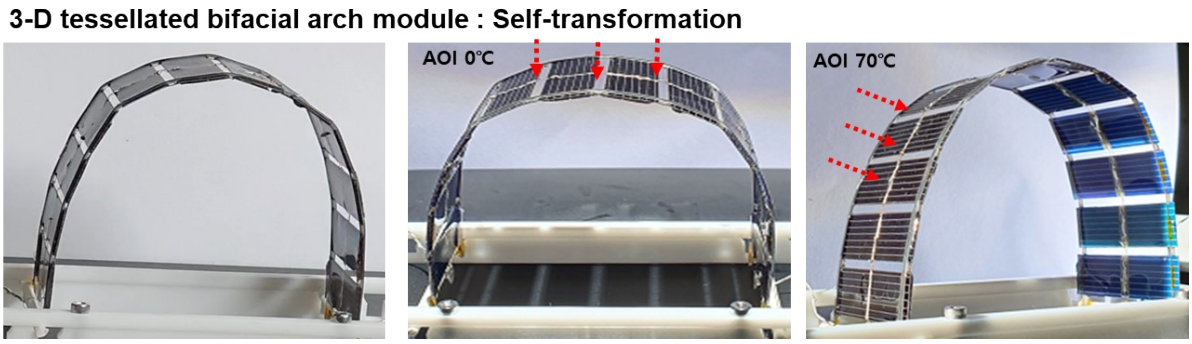


**Figure S19**. Photographs of the self-shape-transformable 3D arch tessellated bifacial module's completed transformed shape under the nonilluminated state (original shape, left), under vertical directional incident light (middle), and under omnidirectional incident light at an AOI of 70° (right).

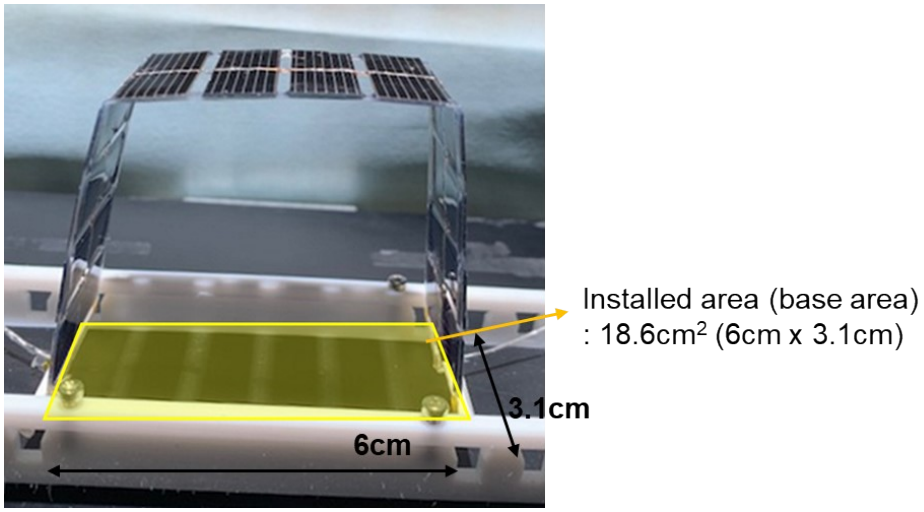


**Figure S20**. Photograph of 3D tetragon tessellated bifacial module and marked installed area (18.6cm$^2$).